Direct correlation of deformation microstructures and cube recrystallization nucleation in aluminium

Adeline Albou, S. Raveendra, P. Karajagikar, Indradev Samajdar, Claire Maurice, Julian Haworth Driver

Direct correlation of deformation microstructures and cube recrystallization nucleation in aluminium

A. Albou,[a] S. Raveendra,[b] P. Karajagikar,[b] I. Samajdar,[b] C. Maurice[a] and J.H. Driver[a,*]

[a] *MPM Department, Ecole des Mines de St Etienne, CNRS UMR 5146, France*
[b] *Department of Metallurgical Engineering and Materials Science, Indian Institute of Technology Bombay, India*

The same section of deformed and annealed Al–0.1 wt.% Mn has been characterized by high-resolution electron backscattered diffraction to determine cube recrystallization nucleation. After 90% plane strain compression, two types of deformed cube segments were present in the microstructure: (i) thin segments along the rolling direction (RD) as "narrow transition bands" between grains; and (ii) fragmented bands inclined about 15° to the RD as "strain localizations" inside grains. On light annealing, cube grains were preferentially nucleated along the intergranular RD segments.

Keywords: Aluminium; Nucleation of recrystallization; Texture; Cube; Cold-rolling

The origin of the cube recrystallization texture is still a source of debate since cube-oriented $(1\,0\,0)\langle 0\,0\,1\rangle$ grains are known to be unstable in cold-rolling [1,2] and the cube component is relatively difficult to observe in the deformed state. In this context, Duggan et al. [3] have pointed out the problem of the "destroyed evidence", i.e. the information loss for the recrystallized nucleus and its environment when analysing microstructures after annealing.

Though it is generally accepted that recrystallized cube grains originate from deformed cube, there are different opinions about the origin of the latter. Following Dillamore and Katoh [4], deformed cube has been postulated to exist as transition bands, i.e. thin cube zones between high orientation gradients created by diverging rotations in unstable orientations. Alternatively, deformed cube has also been proposed as the "fragmented" leftovers of the original cube grains [5]. Though deformed cube has been seen by transmission electron microscopy (TEM) [5–7], its evolution during annealing into cube-recrystallized grains is very difficult, if not impossible, to characterize by TEM.

The resolution improvement of the field emission gun scanning electron microscope (FEG-SEM) now makes the electron backscattered diffraction (EBSD) technique a powerful tool for analysing the heterogeneities of the deformed state. Thus, in a heavily cold-rolled Al alloy it should be possible to observe and characterize different cube bands. Moreover, their evolution during early recrystallization can also be followed by EBSD on the same deformed area to directly characterize the nucleation mechanisms with respect to the initial deformed microstructure – and so get around the "destroyed evidence" problem. The purpose of this work is to characterize cube bands in a deformed model alloy and directly follow their behaviour during light annealing.

Al–0.1 wt.% Mn ingots were processed to obtain an average grain size of 260 μm [8]. This starting material possessed a weak texture ($f_{\max} = 2.6$ characterized by EBSD on over 5000 grains). Samples were deformed in channel die at room temperature to a thickness reduction of 90%. The typical terminology of rolling is used: rolling direction (RD), transverse direction (TD) and normal direction (ND). The deformed microstructure was strongly textured, containing typical β-fibre components of cold-rolled face-centred cubic materials: 48% of S, 38% of Cu, 12% of brass and 1.8% of cube (X-ray orientation distribution function measurements).

Sections from the mid-thickness of the as-deformed samples were mechanically ground and then electropolished. Most of the work was carried out on the standard longitudinal (RD–ND) sections. Some transverse sections (TD–ND) were checked for the deformation microstructure morphology. On the RD–ND sections quick scans were first performed to locate deformed

* Corresponding author. E-mail: driver@emse.fr

cube after making appropriate hardness indentations. The latter acted as markers for EBSD scans after annealing (300 °C 1 h). Scans were made, at a step size of 0.1 μm, at precisely the same area before and after annealing. This enabled a direct microstructural link. It should be noted that previous in-situ annealing studies [9,10] concluded that the free surface has a negligible effect on boundary migration in aluminium. The EBSD measurements were made using TSL-EDX orientation imaging microscopy (OIM) on an FEI Quanta 3D FEG-SEM.

Figure 1a shows an overview of an area containing S, Br and Cu bands together with clearly visible cube segments (highlighted in red) in the deformed state; its structure after annealing is shown in Figure 1b. Texture components within 15° from the ideal orientation are highlighted in greyscale for the main rolling texture components, S, Cu and Br, and also for cube (in red/pink). Table 1 recalls the crystallographic details of these standard orientations. The random texture (Rd) characterizes orientations other than the rolling texture and cube components.

In the deformed state, the overview map presented in Figure 1a can be broken down into four distinct zones of deformed bands: (1) relatively homogeneous S and brass oriented matrices; (2) deformed band containing strain localized bands, inclined about 15° to the RD; (3) stacks of S and Cu bands about 10–20 μm thick; and (4) relatively homogeneous matrices of S oriented grains. The presence of cube components is obvious. They appear as thin elongated bands, either inclined, as in area (2), or horizontal segments. Thick arrows show some locations where thin horizontal cube bands appear lying on boundaries between distinct grains in the area (3) or lying in an S matrix in area (1).

Thus, after observations on both the longitudinal and transverse sections of several deformed samples, two main morphological types of cube bands have been defined: (i) strain-localized cube segments, usually located in a grain of orientation widely spread around $\{1\,1\,0\}\langle 0\,\bar{1}\,1\rangle$; and (ii) cube segments appearing to arise from a transition band, i.e. roughly horizontal bands (or flakes) of thickness 1–2 μm and side lengths of 5–15 μm lying between two distinct grains. An orientation scan across the cube band reveals a very abrupt misorientation change at the interface: >15° over 0.1 μm. Apparently the transition zone was so heavily compressed it condensed into a near grain boundary, so these cube segments are denoted "intergranular".

A minor type has also been observed and consists of a horizontal cube band in an S matrix (in area (1)).

Figure 2 gives more detailed close-up maps of those three kinds of cube bands. In addition, {1 1 1} pole figures are presented to visualize the relationship between the orientations of the different components.

Figure 2a and b presents two examples of strain-localized cube bands inside a highly sheared grain. In Figure 2a, thin elongated cube bands are aligned at an angle of ∼15° to the RD and the surrounding matrix orientation spread is very wide (roughly half the pole figure!). A similar feature is presented in Figure 2b, where thin cube bands are aligned at an angle ±10° to the RD and part of the matrix is near $\{0\,1\,1\}\langle 0\,-1\,1\rangle$.

In general, the majority of the cube transition bands were found on the boundaries between S and/or Cu grains. Two different examples are given in Figure 2c and d. In Figure 2c, cube bands lie on a boundary between two distinct grains of $Rd/Cu_{II}/S_{IV}$ and Cu_I/S_I. From the {1 1 1} pole figure, the two surrounding matrices of Cu and S seem to be related by a rotation around one $\langle 1\,1\,1\rangle$-axis, also common to the cube component. Figure 2d presents a second example of transition cube bands. The surrounding microstructure is more complex and looks like a superposition of thin pancake grains,

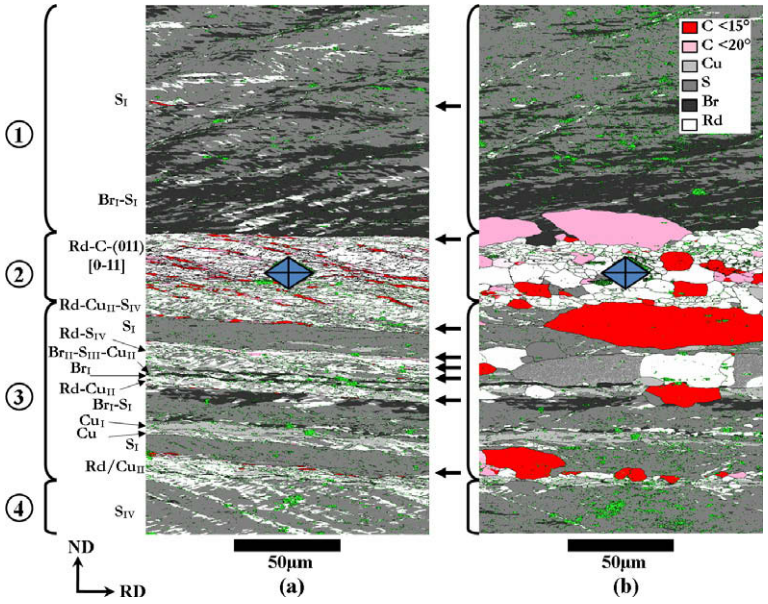

Figure 1. Cube bands (red) in the deformed microstructure (a) and on the same area after 1 h of annealing at 300 °C (b). Main texture components are shown as S, Cu and Br (grey scale) and Rd (white), while arrows point out thin horizontal cubes bands. Non-indexed points are in green. (For interpretation of the references to colour in this figure legend, the reader is referred to the web version of this paper.)

Table 1. β-Fibre and other texture components and related abbreviations.

Texture component	Short form	Miller indices	Texture component	Short form	Miller indices
Cube	C	(1 0 0)[0 0 1]	Random	Rd	–
Brass	Br_I	(0 −1 1)[2 1 1]	S	S_I	(1 2 3)[−6 −3 4]
	Br_{II}	(0 1 −1)[2 1 1]		S_{II}	(1 2 −3)[−6 −3 −4]
Copper	Cu_I	(1 1 2)[1 1 −1]		S_{III}	(1 2 −3)[6 3 4]
	Cu_{II}	(−1 1 2)[1 −1 1]		S_{IV}	(1 2 3)[6 3− 4]
Fibre I: Br_I–S_I–Cu_I			Fibre II: Cu_I–S_{II}–Br_{II}		
Fibre III: Br_{II}–S_{III}–Cu_{II}			Fibre IV: Cu_{II}–S_{IV}–Br_I		

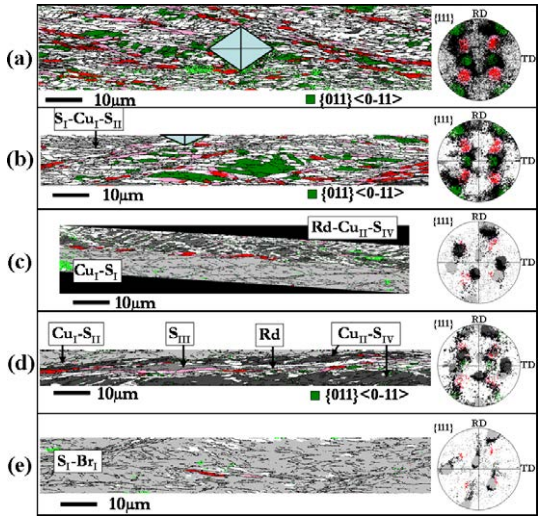

Figure 2. Different morphological types of cube bands in the deformed state: (a and b) strain-localized cube bands; (c and d) transition cube bands; (e) thin cube fragments in S matrix. Cube grains are highlighted in red. {1 1 1} pole figures are presented. (For interpretation of the references to colour in this figure legend, the reader is referred to the web version of this paper.)

containing three types of S- and Cu components. All those components are linked with a common ⟨1 1 1⟩-axis. Moreover, the Rd component seems to be linked to the cube-oriented bands by a lattice curvature about the TD. An initial result of this work is that in practice the orientation of the cube transition surroundings is not symmetrical, in contrast to the Dillamore and Katoh model [4]. A general result is that the cube transition band segments mainly lie between grains of different β-fibre variants.

The third type of cube bands is exceptional and corresponds to a band in a relatively homogeneous S matrix, as shown in Figure 2e (from area (1) in Fig. 1a). Two small elongated cube bands were observed in an S-oriented homogeneous microstructure. Some shear bands are in the vicinity and present a high lattice curvature about the TD (and slightly RD) originated from the S matrix.

The two main types of cube bands are now defined. It is interesting to analyse their behaviour after annealing. As reported by many authors, the cube orientation is well known for having a higher growth rate in the first stage of recrystallization. At first sight, in the annealed sample, the majority (but not all) of the recrystallized grains after 1 h of annealing belong to the cube or near-cube orientations (Fig. 1b). There is also a clear correspondence between the locations of the relatively large recrystallized cube grains and some of the cube fragments in the deformed microstructure. This suggests that the "destroyed evidence" problem has, in part, been overcome by the present method. In part, because one cannot absolutely prove that the cube grains did not originate from beneath the surface. Nevertheless, the concordance between the sites strongly suggests that we are looking at true nucleation sites.

Obviously, the deformed microstructure and its evolution after annealing have to be compared in detail to elucidate the growth mechanisms. Thus, Figure 3 presents some close-ups of the as-deformed and subsequently annealed microstructures.

Figure 3a shows strain-localized cube bands from area (2). All recrystallized grains of this region have approximately the same size. Their orientations retain the orientation range of the deformed state. Thus, after annealing, cube-recrystallized grains are located in the original strain-localized cube bands together with some non-cube-recrystallized grains. It is concluded that, in this particular area, the cube orientation does not have a clear growth advantage since the cube and non-cube grains grow at about the same rates. Some cube impingement (orientation pinning) may also hinder growth here.

The examples of Figure 3b–e are taken from area (3) and show transition bands appearing as horizontal segments between two distinct grains. In these cases, they lie between the S and Cu matrices belonging to different β-fibre variants (but containing some random orientations as well). Moreover, recrystallized cube grains appear after 1 h of annealing at 300 °C exactly in the area where such transition cube bands/segments exist. They seem to grow into the two neighbouring grains but in an anisotropic manner; growth is predominantly along the RD and much less along the ND. However, the size of the recrystallized grain varies substantially from grain to grain: about 80 μm/20 μm for the recrystallized grain in Figure 3b, about 30 μm/15 μm for the recrystallized grains in Figure 3c and d, and very light growth for the grains in Figure 3d (∼5 μm/3 μm). It appears that these types of transition bands act as seeds for the cube-recrystallized grains but their efficiency depends upon the local environment. In particular, it is noteworthy that the fastest growing cube grain in Figure 3b has an orientation relation within 15° of 40°/⟨1 1 1⟩.

Finally, the small cube fragments in the S matrix observed in area (1) vanished completely after annealing. No recrystallized grains were formed in this area. This example reveals that cube fragments in the deformed state are not necessarily the source of recrystallized

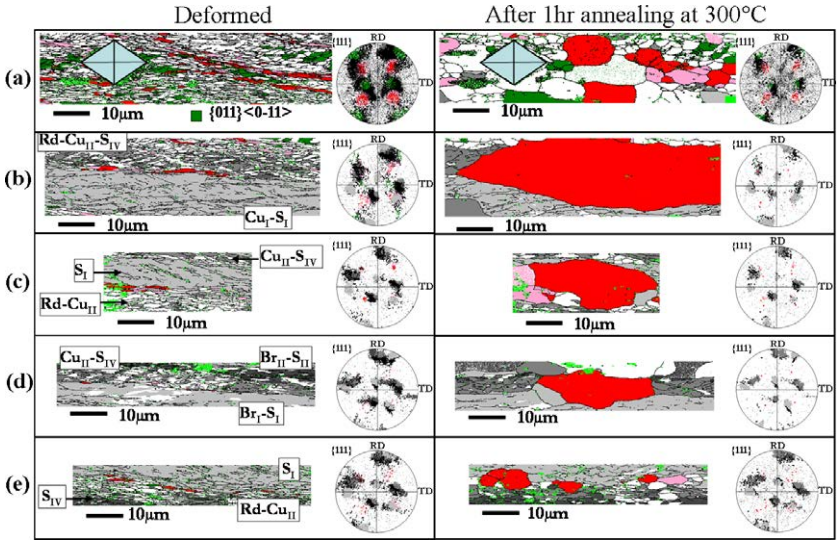

Figure 3. Cube bands in the deformed state and the related annealed microstructure (1 h at 300 °C): strain localized bands (a) and transition bands (b–e). Cube grains are highlighted in red. {1 1 1} pole figures are presented. (For interpretation of the references to colour in this figure legend, the reader is referred to the web version of this paper.)

grains. This assumption is also confirmed when looking at area (3). After annealing, some recrystallized grains of non-cube orientation grew near some cube transition bands.

The existence of a significant density of banded, intergranular cube fragments in cold-rolled Al does not appear to have been clearly identified in previous studies. Here they are clearly the most important sites of recrystallization. The nucleation efficiency of these different types of cube bands has been estimated by comparing the number of cube fragments in the deformed state with the number of recrystallized cube grains from the same sites. This parameter can only be obtained from the type of in-situ annealing observations carried out here to retain the microstructural evidence. An efficiency of about 20% is found for the transgranular "shear band" sites, as opposed to about 40% for the intergranular cube fragments (150 fragments). The higher efficiency of the intergranular segments is almost certainly due to the high local misorientation with the surrounding (S and Cu) grains, which favour the formation, by local sub-boundary coarsening, of high-mobility high-angle grain boundaries.

The origin of the intergranular cube segments in the deformation microstructures is not clear at the moment. The classical models of cube transition band formation by diverging rotations imply symmetrical rotations on either side of the cube band so that it finishes up between two different variants of near-S orientations [4,11]. These symmetrical configurations are not observed here. It is suspected that the intergranular cube segments may be formed at high strains by strain-induced condensation of highly compressed transition zones between β-fibre components. The influence of cold-rolling strain on their formation is currently being studied to clarify their origin.

In conclusion, two major types of thin cube bands have been identified in heavily cold-rolled Al–0.1 wt.% Mn. However, only the intergranular "transition" cube bands led to the formation of high growth rate recrystallized cube grains. The transgranular "strain-localized" cube bands did not lead to a growth advantage for the cube components compared to components of the surrounding matrix. Thus this paper shows explicitly that cube fragments exist in the cold-deformed state in the form of thin horizontal or inclined bands. Observation of the same area with a FEG-SEM after light annealing shows that the horizontal transition band cube segments (usually between different S and Cu oriented grains) lead to cube recrystallization nucleation. Their rate of growth appears to be controlled by their local environments.

Partial financial support was provided by the Indo-French organization IFCPAR under the project "Orientation dependent recovery in metallic materials". The authors acknowledge the National Facility of Texture and Orientation Imaging Microscopy at the Indian Institute of Technology Bombay, India.

[1] F.J. Humphreys, M. Hatherly, Recrystallization and Related Annealing phenomena, second ed., Pergamon Press, Oxford, 2004.
[2] I.L. Dillamore, Ceram. Trans. 201 (2008) 421.
[3] B.J. Duggan, K. Lücke, G. Köhlhoff, C.S. Lee, Acta Metall. Mater. 41 (1993) 1921.
[4] I.L. Dillamore, H. Katoh, Met. Sci. 8 (1974) 73.
[5] I. Samajdar, R.D. Doherty, Acta Mater. 46 (1998) 3145.
[6] A.A. Ridha, W.B. Hutchinson, Acta Metall. 30 (1982) 1929.
[7] Q. Xing, X. Huang, N. Hansen, Metall. Mater. Trans. A 37A (2006) 1311.
[8] F. Barou, C. Maurice, J.-M. Feppon, J.H. Driver, Int. J. Mater. Res. 100 (2009) 516.
[9] Y. Huang, F.J. Humphreys, Acta Mater. 47 (1999) 2259.
[10] A. Lens, C. Maurice, J.H. Driver, Mater. Sci. Eng. A 403 (2005) 143.
[11] F. Basson, J.H. Driver, Acta Mater. 48 (2000) 2101.